An *Ab Initio* Approach Towards Engineering Fischer-Tropsch Surface Chemistry

Type of Report: Technical Progress Report

Report Period: 9/11/2002 - 9/11/2003

Principle Author: Matthew Neurock and Siddharth Chopra

Date: May 01, 2004

DOE Award Number: DE-FG26-01NT41275

Name and Address of Submitting Organization:

Professor Matthew Neurock
Department of Chemical Engineering
102 Engineers' Way
University of Virginia
Charlottesville, VA 22904-4741

DISCLAIMER

I. ABSTRACT

As the US seeks to develop an energy strategy that reduces the reliance on foreign oil, there is a renewed interest in the research and development of the Fischer Tropsch synthesis for converting syngas into long chain hydrocarbon products. This report investigates some of the basic elementary steps for Fischer-Tropsch synthesis over ideal Pt, Ru and carbon-covered Pt and Ru metal surfaces by using ab initio density functional theoretical calculations. We examine in detail the adsorption sites as well as the binding energies for C, CH, CH_2, CH_3 and CH_4 on Pt(111), Ru(0001), 2x2-C-Pt(111) and 2x2-C-Ru(0001). The results indicate that the binding energies increase with decreasing the hydrogen in the fragment molecule, i.e. $CH_4 < CH_3 < CH2 < C_H < C$. More specifically the work analyzes the elementary steps involved in the activation of methane. This is simply the reverse set of steps necessary for the hydrogenation of C to CH_4. The results indicate that these hydrocarbon intermediates bind more strongly to Ru than Pt. The introduction of co-adsorbed carbon atoms onto both Ru(0001) as well as Pt(111) significantly increased the overall energies as well as the activation barriers for C-H bond activation. The results suggest that Ru may be so active that it initially can initially activate CH_4 into CH or C but ultimately it dies because the CH and C intermediates poison the surface and thus kill its activity. Methane can dissociate on Pt but subsequent hydrocarbon coupling reactions act to remove the surface carbon.

II. TABLE OF CONTENTS

III. INTRODUCTION

The past decade has witnessed a strong revival of both hydrocarbon reforming as well as Fischer-Tropsch synthesis as critical processes necessary for in the production of hydrogen for fuel cell applications and synthesis gas which can be used to cleanly produce petroleum products. Fischer-Tropsch synthesis (FTS) is a catalytic process that converts synthesis gas (a mixture of CO and H_2) to useful hydrocarbon products and synthetic fuel/oil free of sulfur, nitrogen and metal contaminants. Since FTS has a potential to reduce the dependence on crude oil for producing fuels there has been a growing interest in the research and development of FT related processes.

The overall process of FT synthesis is comprised of a complex network of elementary bond-breaking and bond-forming steps. These steps include CO and H_2 activation as well as hydrogenation and chain growth over supported metals. A schematic of the surface processes that are thought to occur is shown in Figure 1. The balance of the bond breaking and bond formation steps controls the reactivity and selectivity of the process. For example, transition metals to the left in the periodic table will readily activate CO but the products, i.e. surface carbon and oxygen, are too strongly bound to the surface, thus blocking subsequent hydrogenation and carbon coupling reactions. Transition metals to the right, on the other hand, are not active enough to dissociate CO[1,2]. The ideal catalysts for FT synthesis would be those metals that can promote CO activation, along with a balanced degree of surface hydrogenation and hydrocarbon coupling in order to produce longer chain hydrocarbon products. Therefore, analyses of the elementary steps involved in the reaction are important in the search for the best catalysts and the optimal operating conditions.

Over the past 70 years since Fischer and Tropsch discovered this process, there have been a large of number of research studies on the mechanism and the optimal operating conditions to form the desired products[3-7]. Studies on syntheses and characterization of the different catalysts have provided essential information for catalyst development and industrial reactor design. However, a fundamental understanding of the how the atomic surface structure of the catalyst controls the elementary molecular transformations in FT catalysis is still poorly understood.

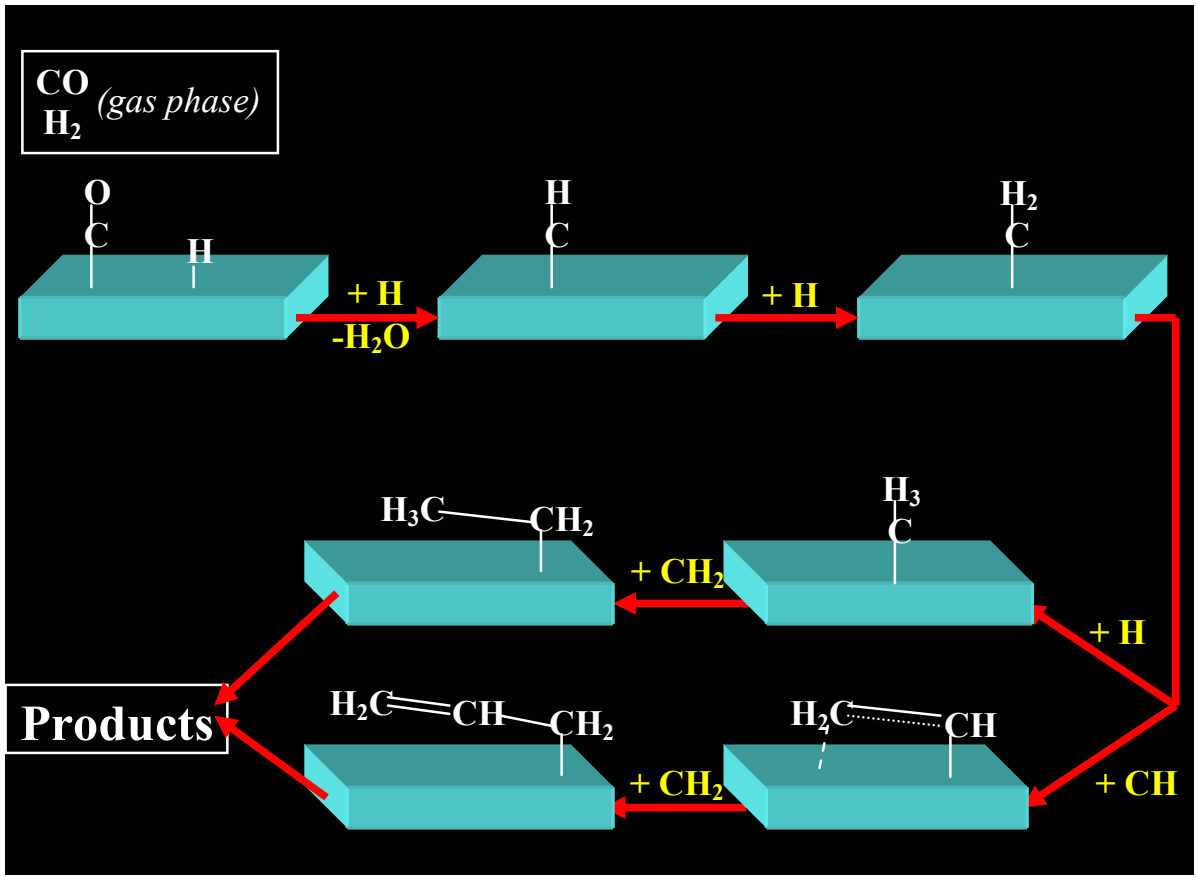

Figure 1: Schematic of elementary surface reaction steps in FT synthesis

In the present project, we use *ab initio* quantum mechanical methods to analyze the elementary surface steps over model surfaces involved in FT chemistry. The aim of this project is to gain

insight of the reaction mechanisms and to elucidate the structure features that control catalytic performance through a detailed analysis of the elementary steps involved in the process. In year one of the project, we analyzed CO activation as well as hydrocarbon coupling over model Co(0001) and corrugated Co surfaces in order to understand their role in the mechanism. In year two, we have examined the coupling of hydrocarbon chain fragments of Co(0001) and Ru(0001) surfaces.

In this past year we have extended our mechanistic understanding for the hydrogenation of CH_x intermediates on Co. More specifically we have calculated the reaction energies and activation barriers for the hydrogenation of CH_x intermediates over model Co, Ru, Rh and Pt model closed packed surfaces. We have also analyzed the effect of the presence that surface carbon has on each of these CH_x hydrogenation steps on Pt(111) and Ru(0001) surfaces.

IV. EXECUTIVE SUMMARY

The past decade has witnessed a renewed interest in Fischer-Tropsch (FT) synthesis as a process critical in the conversion of methane to liquid fuels and the clean processing of coal to chemicals and energy. Fischer-Tropsch synthesis involves a complex but tightly balanced scheme of bond making and breaking processes including the activation of CO and H_2, the hydrogenation of hydrocarbon fragments, the coupling of hydrocarbon surface intermediates, and desorption of longer chain hydrocarbon products. The ideal catalysts for FT synthesis would be those metals that can promote CO activation, along with a balanced degree of surface hydrogenation and hydrocarbon coupling in order to produce longer chain hydrocarbon products. An understanding of the elementary steps involved in the reaction is therefore important in the search for the best catalysts and the optimal operating conditions. Despite years of research, the fundamental understanding of the how the atomic surface structure of the catalyst controls the elementary molecular transformations in FT catalysis is still poorly understood.

We have used *ab initio* quantum mechanical methods to analyze the elementary surface steps over model transition metal surface in order to help elucidate reaction mechanisms. In the first year of this project, we analyzed in detail the activation of CO over Co(00001) and stepped Co single crystal surfaces to establish the influence of the surface corrugation and openness on the energetics. In addition, we probed the effect of coverage on the calculated energetics. Both surface structure as well as coverage were found to have a significant effect. In year two of the project we focused on relevant CH_x hydrocarbon coupling pathways. Our results suggest that both CH_2 and CH may be kinetically important intermediates.

In this past year we have examined in detail the decomposition of methane to CH_x intermediates along with the reverse process, the hydrogenation of CH_x intermediates to methane. We have calculated the reaction energies and activation barriers for both C-H bond breaking and bond making for all of the C_1H_x intermediates over model Ru and Pt (for comparison with our previous results on Co(0001)) closed packed surfaces in order to elucidate periodic trends. In addition to the intrinsic energetics, we have also explored the effect that surface carbon has on each of these CH_x hydrogenation steps on Pt(111) and Ru(0001) surfaces.

We focus here on a comparison of the energies for the activation of methane on Pt(111) and Ru(0001) surfaces in both the absence and the presence of adsorbed surface carbon. This is simply the reverse of the hydrogenation reaction necessary for FT. Recent results from Iglesia (J. Phys. Chem. B, 108, 13, 4094, 2004) indicate that methane activation occurs more readily on metals further to the right in the periodic table. Surface science results over ideal single crystals however show the opposite behavior. Our results show that the overall reaction energies as well as the activation barriers for methane activation are higher on metals that lie to the right (Pt) in the periodic table. The values for the overall reaction energies however on the ideal surfaces Pt(111) and Ru(0001) surfaces at low coverages are +1 Pt (-6 Ru), +24 Pt (-11 Ru), -23 Pt (-56 Ru), and +38 (-21 Ru). This behaves according to simple d-band filling model which suggests that the reaction should become more exothermic (less endothermic) in moving from right to left in the periodic table which would agree with surface science results. We show very similar trends for the calculated activation energies. This, however, is inconsistent with the experimental results by Iglesia. One possible explanation is that Ru may be so active that it can

actually form a carbidic overlayer which should reduce its reactivity. Subsequent methane activation steps were carried out over a surface which was covered with 0.25 ML of preadsorbed carbon atoms. The overall reaction energies for CH_4 -> $CH3_{4-x} + H_x$ were –1 Pt (0 Ru), 49 Pt (45 Ru), +49 Pt (+41 Ru), 113 (19 Ru), 141 (+19 Ru) and 261 Pt (81 Ru) kJ/mol respectively. The overall energies are clearly more endothermic than those on the bare surfaces. Ru(0001) however still appears to be more active than the Pt(111). A comparison of the activation barriers shows similar trends.

The emerging picture is that Ru may be so active that it readily activates CH_4 into CH or C intermediates which are difficult to remove and thus poison the surface. On Pt, methane dissociates but subsequent hydrocarbon coupling reactions act to remove the surface carbon.

V. COMPUTATIONAL METHODS

The work described herein was carried out using plane-wave density functional periodic slab calculations as implemented in the VASP code developed by Kresse and coworkers[8-13]. The electron-ion interactions were described by ultra-soft pseudopotentials[14] with a plane-wave cut off energy of 287 eV. The Perdew-Wang form (PW91) of general gradient corrections was used to calculate the exchange and correlation energies[15]. The surface was modeled by using 2x2 supercells having 4 metal layers. The Monkhorst-Pack[16] mesh was used to sample the surface Brillouin zone. Throughout our calculations, we used a one-sided slab approach, i.e. placing adsorbates on one side of the slab. The atoms of the adsorbates and those in the top two layers of the metal slab were allowed to optimize according to the forces calculated quantum mechanically.

Transition states were isolated using the Nudged Elastic Band (NEB) method developed by Jonsson and coworkers[17] as implemented in VASP.

VI. RESULTS AND DISCUSSION

1) Bulk Structures of Pt and Ru

The bulk metal lattice parameters along and resulting electronic properties were calculated for each metal prior to any surface calculations. The calculated lattice constants for bulk Pt and Ru are listed in Table 1. The lattice constant for Co was calculated earlier.

Table 1: Calculated Pt and Ru bulk lattice parameter, a(A°)

	Pt	Ru
Theory	2.822	2.730
Exptl.	2.772	2.71

2. Hydrogenation of Surface CH_x species

The hydrogenation and dehydrogenation of the CH_x species over the active metal surface is essential for understanding the operative mechanism(s) for FTS. Both the forward steps for the hydrogenation of C_1 to CH_4, as well as the reverse dehydrogenation steps, have been studied in detail. The synthesis of longer chain hydrocarbons in FTS requires an optimal balance between hydrogenation and hydrocaron chain coupling. The hydrogenation of different surface carbon intermediates all the way to methane is undesirable. These CH_x intermediates should be mobile on the surface[18] and thus act as monomer units in the propagation of the growing hydrocarbon chain. An analysis of the reaction energies for these elementary steps also aids in understanding the relative thermodynamic stability of the CH_x species on the surface. We examine here both the hydrogenation and dehydrogenation processes over close-packed Pt(111) and Ru(0001) surfaces as part of the ongoing effort to understand trends in the behavior of metals across the periodic table.

There is a wealth of fundamental literature on the activation of methane over well-defined single crystals. This provides insight not only into the dehydrogenation paths but the hydrogenation paths as well. Different forms of carbonaceous species are known to be present on a metal during both methane activation as well as the hydrogenation of carbon monoxide on Group VIII

metals[19-22]. These forms differ in their kinetics of formation and in their reactivity. C_α is a highly reactive form and is the principal intermediate in the synthesis of methane and C_{2+} hydrocarbons[20]. It has been identified as a carbidic (atomic) type of carbon by surface characterization techniques such as AES and SIMS. C_β is less reactive than C_α and is formed from C_α in the presence of surface hydrogen[22]. C-H, C-C and C-M interactions are present in C_β and so it is supposed to exist as an amorphous phase[20]. Since the elementary steps involved in methane dissociation over the metal surface occurs in the presence of these carbon forms, the effect of lateral interactions from these surface species need to be considered. To understand this effect we studied the elementary steps in the presence of surface bound carbon atoms which have been used to represent the surface carbon forms.

3) CH_x chemisorption and CH_4 decomposition path on Pt(111)

The preferred binding sites, their corresponding binding energies and Pt-C bond lengths for all of the C_1H_x adsorbed on Pt(111) were calculated and are summarized in Table 1. On Pt(111) we found that the CH_x species binds at sites so as to maintain an sp^3 or tetrahedral configuration. Every C-H bond that breaks appears to be substituted with a single C-M bond where M is a surface metal atom, thus maintaining four σ bonds to the carbon. Thus, CH_3 prefers to sit atop a single metal atom, CH_2 prefers to sit at a bridge site forming two σ bonds with the two metal atoms, while CH and C prefer fcc hollow sites forming three σ bonds with the three metal atoms. As expected, the binding energies were found to increase in the order:

$$CH_3 < CH_2 < CH < C$$

which correlates with the increasing number of Pt atoms coordinated with the C. The Pt-C bond length decreases with the number of Pt-C bonds. The preferred binding sites along with the calculated Pt-C bond lengths for these same CH_x intermediates on Pt(111) in the presence of nearest neighbor surface carbon are shown in the lower half of Table 1. The Pt-C bond is slightly increased in the presence of other surface carbon. This is expected since the binding energy becomes weaker due to repulsive lateral interactions between the surface CH_x and the preadsorbed carbon. The C-H bond length for nearly all of the intermediates was found to be fairly constant around 1.1 A°.

Table 2: CHx Binding Data on Pt(111) and C_Pt(111) for 25% coverage

Pt(111)

Species	CH3	CH2	CH	C
Adsorption site	atop	bridge	fcc	fcc
Pt-C (A°)	2.074	2.054	2.004	1.920
BE (kJ/mol)	-198.0	-399.0	-634.4	-674.3

C_Pt(111)

Species	CH3	CH2	CH	C
Adsorption site	atop	bridge	fcc	fcc
Pt-C (A°)	2.089	2.040, 2.078	2.021, 2.021, 1.964	1.985, 1.987, 1.895

The overall reaction energies for methane decomposition over Pt(111) are shown in Figure 2. The hydrogenation of C to CH_4 is simply the reverse path which can be determined from Figure 2 by following from right to left in the figure instead of left to right. The energies of

the CH_x + (4-x) H_x (x=0-4) states shown in the figure have been calculated *relative to the energy of methane in the gas phase*.

They are calculated by adding (4-x) times the energy of the adsorbed hydrogen atom to the energy of CH_x species in the gas phase and subtracting the result from the total energy for the adsorbed CH_x system. The reaction energy of the elementary step $CH_{x+1} \rightarrow CH_x + H$ corresponds to the difference in the energies of two successive states shown in the figure. Since these energies have been determined at a coverage of 25% they include some degree of lateral interactions between the adsorbates. Also, the energies correspond to the most favored adsorption geometries for CH_x and H on Pt(111) which have been shown in Figure 3. All the dissociation steps, with the exception of $CH_2 \rightarrow CH+H$, were found to be endothermic on Pt(111). The overall reaction energies provide an idea about the relative thermodynamic stability for each of the CH_x species on the surface. CH seems to be the most stable among the C_1 species on the surface.

The hydrogenation for the CHx intermediates to methane follows the reverse reaction path in Fig. 2.

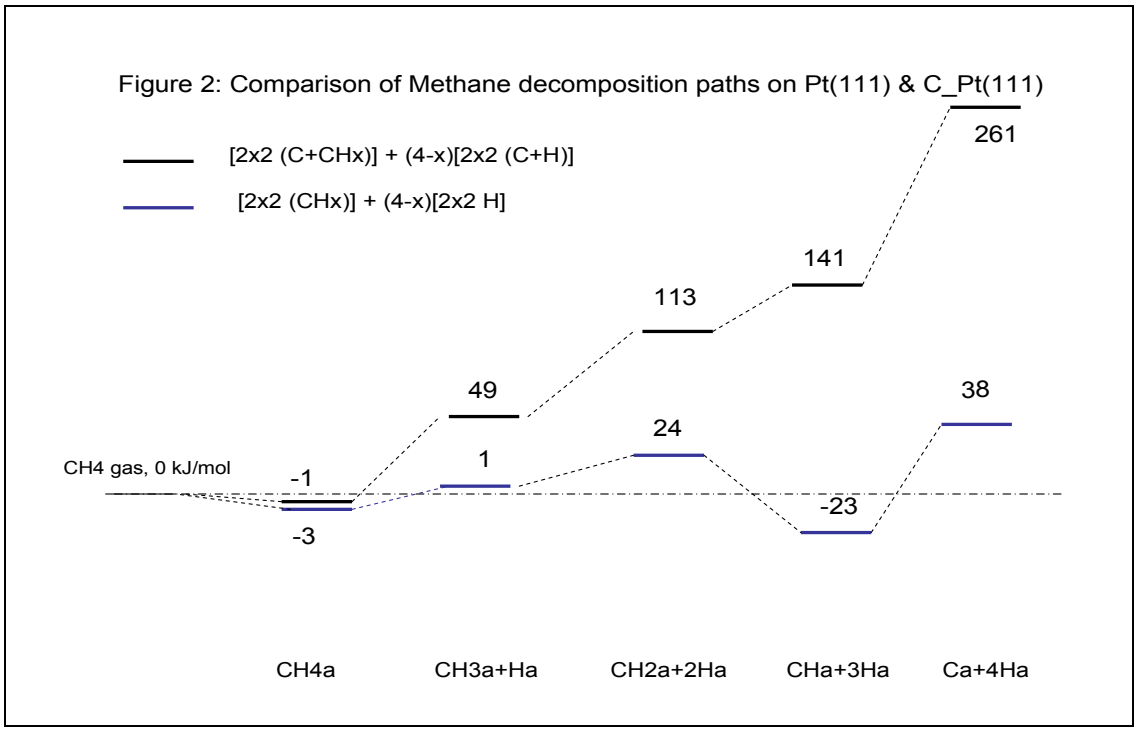

These same reactions were subsequently examined in the presence of adsorbed atomic carbon in order to begin to understand the influence of the coverage of CH_x intermediates and dehydrogenated hydrocarbon fragments on the overall surface reactivity. The overall reaction energies for methane activation change significantly in the presence of surface carbon. These energies, once again, correspond to the most favored adsorption geometries for carbon and CH_x coadsorbed on the surface (Figure 4). The binding energies for each CH_x species were found to be weaker on the Pt(111)-C surface than they were on the clean Pt(111) surface. This is due to the repulsive interactions between the adsorbed CH_x species and the surface carbon. Also, there was a change in the relative stability of the CH_x species. CH_3 and CH_2 appear to be the more stable than CH on the carbon covered surface.

Activation barriers were also calculated for the elementary C-H bond activation steps $CH_{x+1} \rightarrow CH_x + H$ (x=0-3) on Pt(111). These energy barriers include the some degree of lateral interaction

between the CH_x as they correspond to a coverage of 25%. The transition state structures were shown in Figure 3. From the NEB calculations we found that the hydrogenation steps for the formation of CH and CH_4 have lower activation barriers. The activated bond in the transition state for these steps lies at the atop position which leads to stabilization due to increased overlap with the metal orbitals. On the other hand, the barriers for the formation of CH_2 and CH_3 are greater because of greater geometrical distortion of the transition state.

Figure 3:Transition States & Activation Energies on Pt(111)

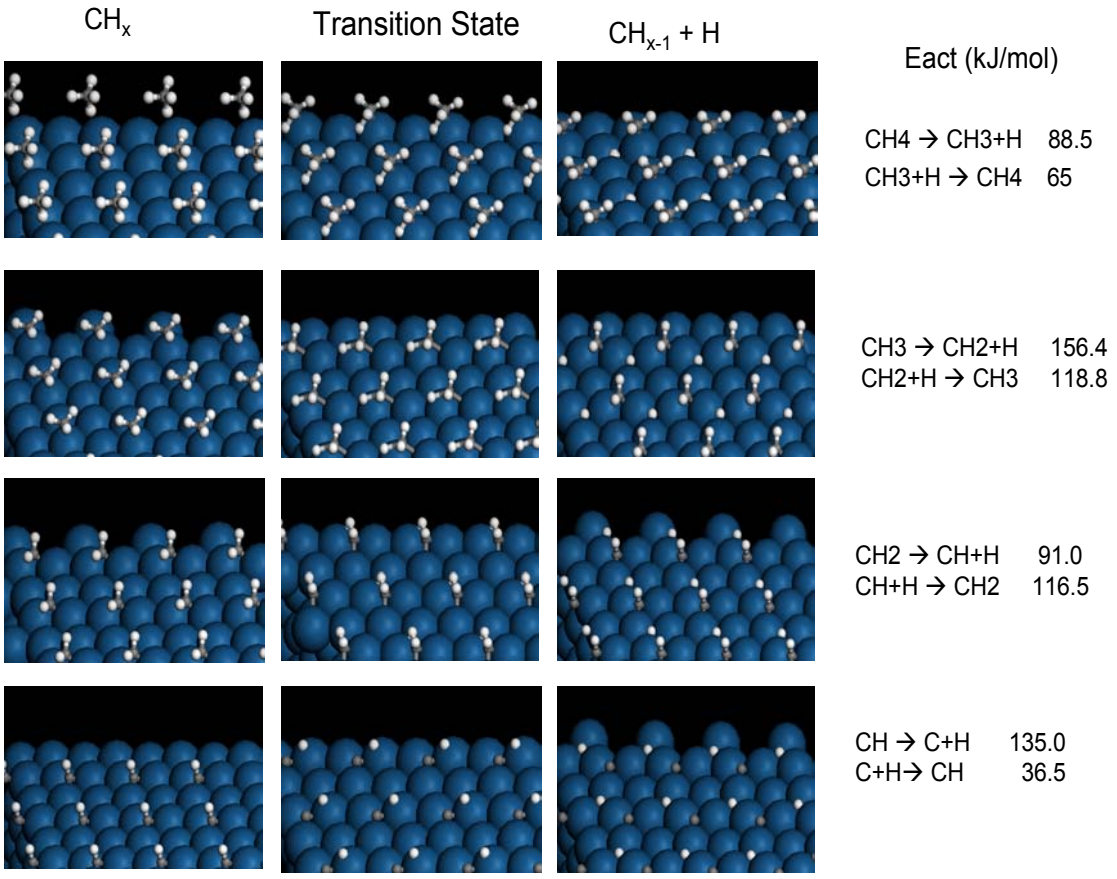

Figure 4: Most favored geometries of CHx, H in the presence of C on Pt(111)

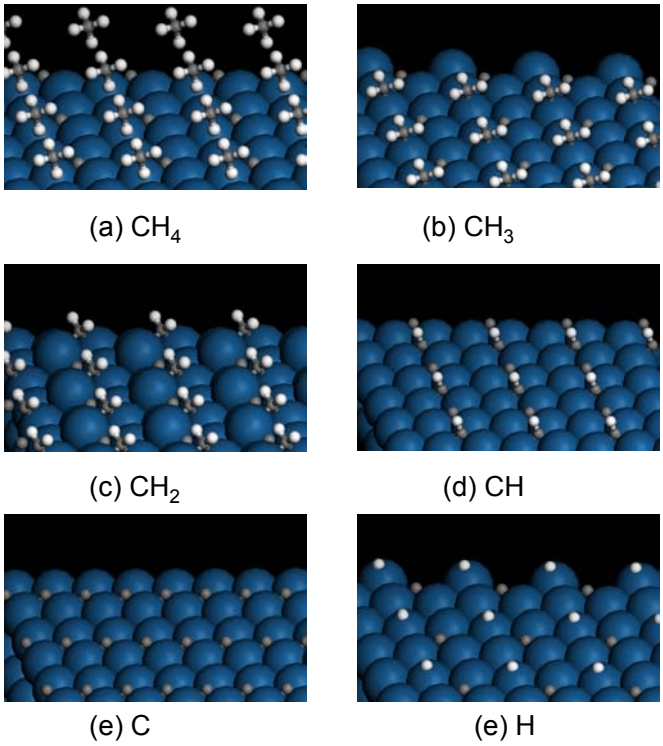

(a) CH_4 (b) CH_3

(c) CH_2 (d) CH

(e) C (e) H

4) CH_x chemisorption and CH_4 decomposition path on Ru(0001)

The preferred binding sites and the binding energies for CH_x adsorbed on the Ru(0001) surface are shown in Table 3. All of the CH_x intermediates prefer to bind at the hollow sites on Ru(0001). While CH_3 prefers the fcc hollow site, CH_2, CH, and C prefer to bind at hcp hollow sites[23]. As in the case of Pt(111), the binding energies increase and the Ru-C bond lengths decrease with a decrease in the number of hydrogen atoms (CH_3 < CH_2 < CH < C). The Ru-C bond lengths varied in the range 1.7 to 2.2 A° while C-H distances were around 1.1 A° for all the intermediates[23]. The CH_x binding energies on Ru(0001) are significantly stronger than those on Pt(111). This is to be expected since Ru has more vacancies in its d-band than that for Pt.

Table 3: CHx Binding Data on Ru(0001) and C_Ru(0001) for 25% coverage

Ru(0001) *

Species	CH3	CH2	CH	C
Adsorption site	fcc	hcp	hcp	hcp
BE (kJ/mol)	-198.8	-409.5	-641.96	-688.34

C_Ru(0001)

Species	CH3	CH2	CH	C
Adsorption site	atop	hcp	hcp	hcp
Ru-C (A°)	2.169	2.061,2.062, 2.236	2.023, 2.027, 2.003	1.954, 1.953, 1.900

* Ref. 23

The decomposition of methane over Ru(0001) was established earlier by Ciobica et al. [23] who carried out similar calculations is presented at the top of Fig. 5. Our results for methane activation over a carbon covered Ru(0001) surface are shown in the lower half of Fig. 5. The DFT-optimized geometries for the CH_x species adsorbed on Ru(0001) in the presence of carbon are shown in Figure 6. The binding energies for all of these intermediates are considerably lower than the binding energies on the 2x2 carbon covered Ru(0001) surface. All of the elementary C-H activation steps, with th exception (CH→ C+H), were found to be exothermic over the Ru(0001) surface. The overall reaction energies for each C-H activation step were considerably higher and predominantly endothermic on the 2x2 carbon covered Ru(0001) surface. This is primarily due to repulsive lateral interactions between the surface

CH_x intermediates and coadsorbed carbon atoms. Amongst the CH_x species, CH appears to be the most stable species on the surface which is in good agreement with the experimental study by Wu and Goodman[18] in which they looked at hydrocarbon formation from methane decomposition on Ru(0001). Our results suggest that CH should be a key monomer unit that can combine with the growing hydrocarbon chain under FT conditions. A more complete analysis however will require full kinetic simulations of the all of the surface processes.

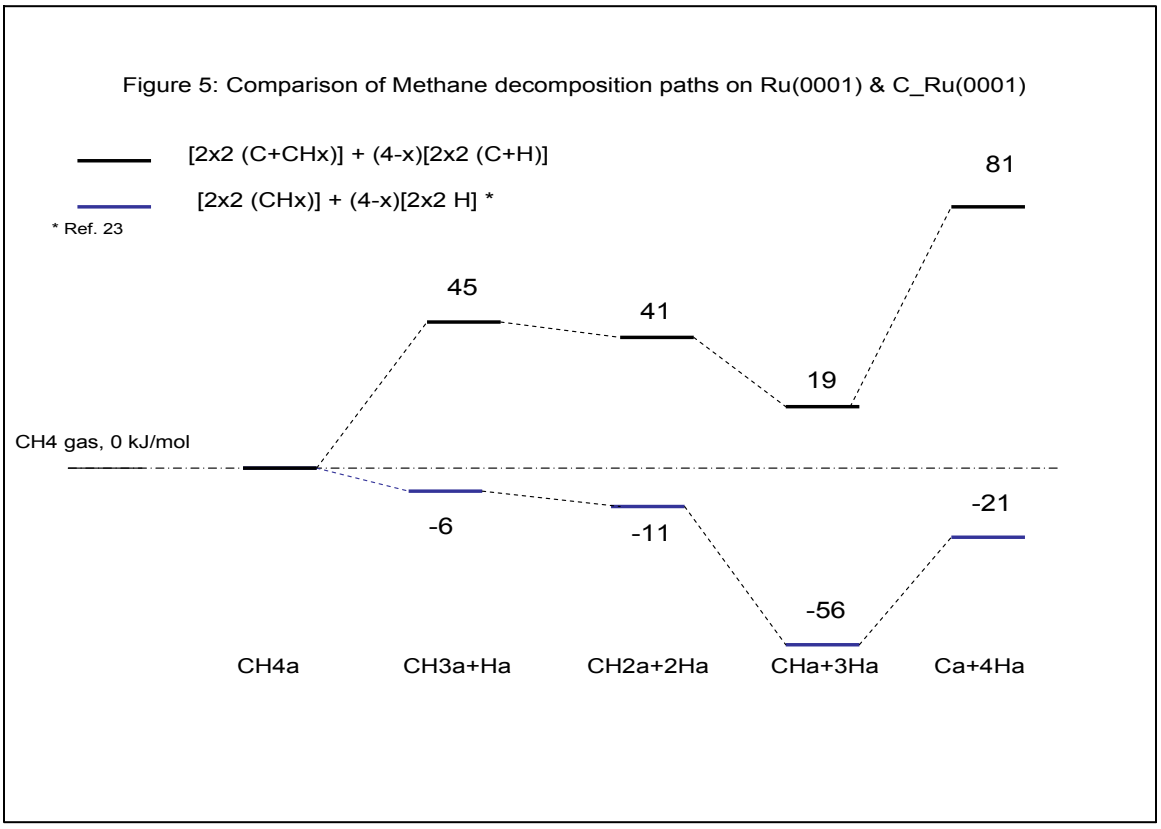

Figure 5: Comparison of Methane decomposition paths on Ru(0001) & C_Ru(0001)

Figure 6: Most favored geometries of CHx, H in the presence of C on Ru(0001)

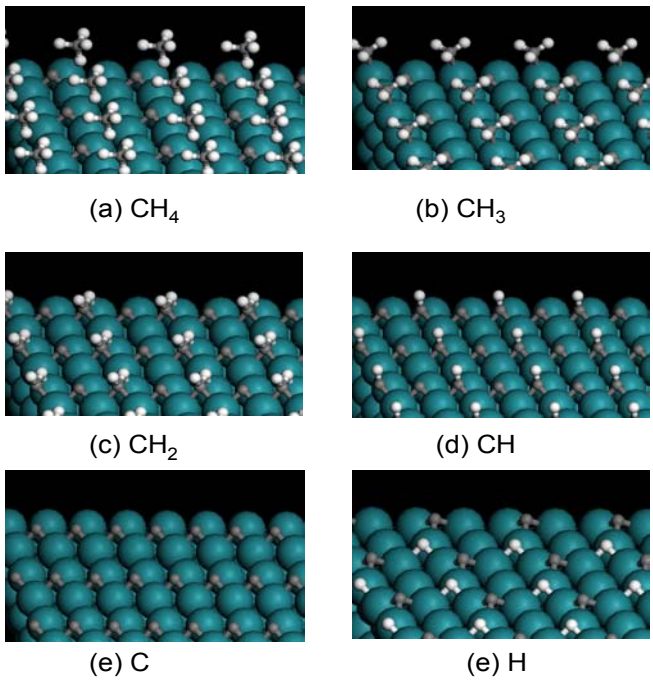

(a) CH_4 (b) CH_3

(c) CH_2 (d) CH

(e) C (e) H

VII. CONCLUSION AND FUTURE EFFORTS

The results from ab initio quantum chemical calculations indicate that methane activation is more favorable over Ru than Pt. The overall reaction energies become more exothermic in moving from Pt to Ru. The calculated overall reaction energies for the C-H activation of CH4, CH3, CH2 and CH, at low coverages over Pt(111) and Ru(0001) were calculated to be: +1 Pt (-6 Ru), +24 Pt (-11 Ru), -23 Pt (-56 Ru), and +38 (-21 Ru) respectively. The activation barriers also decrease in moving from Pt(111) to Ru(0001). This behaves according to simple d-band filling model which suggests that the reaction should become more exothermic (less endothermic) in moving from right to left in the periodic table. The presence of surface carbon dramatically lowers the favorability for the activation of methane over both Pt as well as Ru. The overall

reaction energies for CH_4 -> $CH3_{4-x}$ + H_x on the carbon covered surfaces were calculated to be: –1 Pt (0 Ru), 49 Pt (45 Ru), +49 Pt (+41 Ru), 113 (19 Ru), 141 (+19 Ru) and 261 Pt (81 Ru) kJ/mol respectively. The results suggest that hydrocarbon fragments that form on Ru are significantly more stable than those on Pt. If these species form on Ru they likely will lead to site blocking. Their intermediate strength on Pt may allow them to be ultimately removed from the surface.

Future efforts will examine the influence of surface oxygen and water and their role in methane activation and Fischer-Tropsch synthesis. In addition, the results from all of our previous theoretical calculations will be used in building a first-principles-based kinetic Monte Carlo simulation to examine the initial stages of Fischer-Tropsch synthesis.

References

[1] Horn, K.; Bradshaw, A.; Jacobi, K. *Surf. Sci*. **1978**, 72, 719.

[2] Vannice, M. A. In *Catalysis: Science and Technology, Vol. 3.* Springer-Verlag, Berlin, **1982**; chapter 3.

[3] Anderson, R. B. *The Fischer-Tropsch Synthesis*, Academic Press, New York, **1984**.

[4] Iglesia, E.; Reyes, S. C.; Madon, R. J.; Sloled, S. L. *Adv. Catal.* **1993**, 39, 221-302; Iglesia, E. Appl. Catal. **1997**, 161, 59-78.

[5] Thomas, J. M.; Thomas, W.J. *Principles and Practices of Heterogeneous Catalysis*; CH: Weinheim, **1997**.

[6] Dry, M. E. *Catal. Today*, **2002**, 71, 227-241.

[7] Van der Laan, G. P.; Beenackers, A. A. C. M. *Catal. Rev. – Sci. Eng.*, **1999**, 41, 255-318.

[8] Payne, M.C.; Teter, M.P.; Allan, D.C.; Arias, T.A.; Joannopoulos, J.D. *Rev. Mod. Phys*. **1992,** 64, 1045-1097.

[9] Kresse, G.; Hafner, J. *Phys. Rev. B* **1993**, 47, 558-561

[10] Kresse, G.; Hafner, J. *Phys. Rev. B* **1994**, 49, 14251-14269

[11] Kresse G. a. J.F. *Comp. Mat. Sci.* **1996**, 6, 15-50

[12] Kresse, G.; Furthmuller, J. *Phys. Rev*. B **1996**, 54, 11169-11186

[13] Kresse, G.; Furthmuller, *Comp. Mat. Sci.* **1996**, 6, 15

[14] Vanderbilt, D. *Phys. Rev. B* **1990**, 41, 7892.

[15] Perdew, J.P.C., J.A.; Vosko, S.H.; Jackson, K.A.; Pederson, M.R.; Singh, D.J.; Frolhais, C. *Phys. Rev. B* **1992**, 46, 6671-6687

[16] Monkhorst, H.J.; Pack, J.D. *Phys. Rev. B* 1976, 13, 5188-5192

[17] Mills, G.; Jonsson, H.; Schenter, G.K. *Surf. Sci*. **1991**, 324, 305

[18] Wu, M.; Goodman, D.W. *J. Am. Chem. Soc.* **1994**, 116, 1364-1371

[19] Koerts, T.; van Santen, R.A. *J. Chem. Soc., Chem. Commun.* **1991**, 1282

[20] Koerts, T.; Deelen, M.J.A.G.; van Santen, R.A. *Journal of Catalysis* **138**, 101 -114

[21] Winslow, P.; Bell, A.T.; *Journal of Catalysis* **91**, 142-154

[22] Duncan, T.M.; Winslow, P.; Bell, A.T. *Journal of Catalysis* **93**, 1-22

[23] Ciobica, I.M.; Frechard, F.; van Santen, R.A; Kleyn, A.W.; Hafner, J. *Chem. Phys. Lett.* **1999**, 311, 185-192